

Thermoelectric Power of Vacancies in Aluminum*

Theodore Rybka and Ronald R. Bourassa

Department of Physics and Astronomy, University of Oklahoma, Norman, Oklahoma 73069

(Received 29 March 1973)

The thermoelectric potential difference between a well-annealed aluminum wire and a quenched aluminum wire has been measured as a function of temperature from 4 to 150 °K. Measurements were made for several quench temperatures and for a distilled ice and water quench followed by rapid insertion into a dry ice and methanol medium. These data were used to determine the effect of vacancies on the thermopower of aluminum. The thermopower is enhanced by vacancies at temperatures below about 70 °K and reduced at higher temperatures. It is proposed that the enhancement is due to the change in electron-diffusion thermopower. A calculation of this effect has been made based on the theory of Nielsen and Taylor, and the agreement with the experimental results is striking. The reduction in thermopower above 70 °K is explained by the change in the phonon-drag thermopower due to vacancies. The Rayleigh-scattering parameter was determined from the experimental data and is compared to calculated values using the theories of Klemens and Carruthers.

I. INTRODUCTION

The absolute thermopower S of a pure metal consists of an "electron diffusion" contribution S_e , arising from the nonequilibrium distribution of the conduction electrons, and a "phonon-drag" contribution S_g , caused by the interaction between the conduction electrons and the phonons which are not in equilibrium:

$$S = S_e + S_g. \quad (1)$$

The introduction of defects into a metal causes a change, ΔS_e and ΔS_g , respectively, in both contributions. The change in S_e depends only on the electron scattering properties and on the electronic band structure of the system. The absolute magnitude of S_g is normally reduced because the additional phonon scattering by the defects reduces the phonon current set up by the temperature gradient. Possible exceptions to this were found in 1966 by Farrell and Greig,¹ in 1967 by Van Baarle² and Guenault,³ and in 1968 by Huebener⁴ when he measured the thermopower of dilute alloys of aluminum. Huebener's data for the thermopower of the alloy Al+0.03-at.% Zn versus pure aluminum is shown as a function of temperature in Fig. 1. The convention is such that positive values of S indicate a reduction in the thermopower of aluminum due to the impurities while negative values indicate an enhancement. ΔS is the total change in thermopower due to impurities and can be written

$$S = \Delta S_e + \Delta S_g. \quad (2)$$

Huebener calculated ΔS_e using the theories available in 1968 and found it to be positive at all temperatures. This led him to conclude that at low temperatures ΔS_g was negative, implying that alloying aluminum increased the phonon-drag component of thermopower.

Semiquantitative treatments of these anomalies in the phonon drag contributions have been developed by Van Baarle,² Fletcher and Dugdale,⁵ Bailyn,⁶ and Dugdale and Bailyn.⁷ They have shown that anomalies in the low-temperature phonon-drag thermopower in impure systems can occur if the relaxation time for the electron scattering by impurities and the relaxation time for the electron scattering by phonons vary differently over the Fermi surface. Huebener was able to use these ideas to qualitatively explain the low-temperature enhancement of the thermopower of aluminum on alloying.

From 1968 to 1970 Nielsen and Taylor⁸⁻¹⁰ developed a new theory of electron-diffusion thermo-

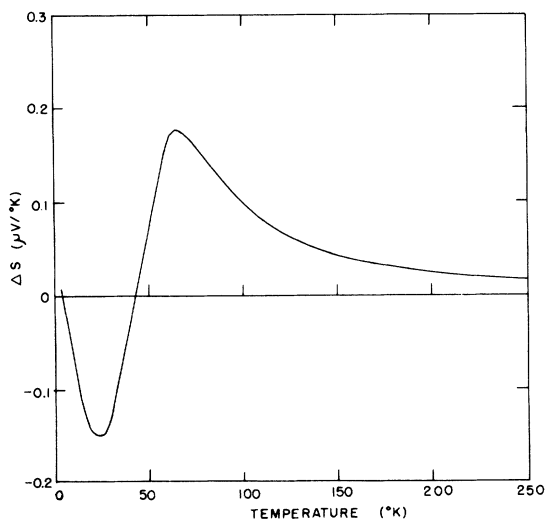


FIG. 1. Thermopower of the alloy Al+0.03-at.% Zn. (Taken from Huebener, Ref. 1.)

power which was applied to aluminum alloys by Dudenhoeffer and Bourassa.¹¹ The new theory provided a relatively simple explanation for Huebener's experimental data on aluminum alloys, namely that the low-temperature negative peak in ΔS was due to ΔS_e as calculated now using the Nielsen-Taylor theory and that the high-temperature positive peak was due to ΔS_ζ .

The importance of determining the validity of the Nielsen-Taylor theory is readily apparent when one realizes that most published thermopower work involves a separation of the electron-diffusion component from the phonon-drag component. If the Nielsen-Taylor theory is valid, that separation has been made incorrectly in the past.

In this experiment the difference in thermoelectric voltage between a well-annealed aluminum wire and an aluminum wire containing vacancies was measured as a function of temperature from 4.2 to 150°K, and the difference in thermopower, ΔS , between the two wires was determined. The Nielsen-Taylor theory as well as phonon-drag theory were used in analyzing the results.

II. THEORY

Thermopower Relationships

The electron-diffusion thermopower of a metal is given by

$$S_e = -S_0 \left(\frac{\partial \ln \rho(\epsilon)}{\partial \ln \epsilon} \right)_\zeta, \quad (3)$$

$$S_0 = \pi^2 k_B^2 T / 3e\zeta, \quad (4)$$

where e is the (negative) electronic charge, k_B is Boltzmann's constant, T is the absolute temperature, ϵ is the hypothetical height of the Fermi level, ζ is the Fermi energy, and $\rho(\epsilon)$ is the electrical resistivity of the metal evaluated at ϵ .

In dilute metallic systems the crystal defects can be treated approximately as independent so that the resistivity ρ of the system is given by the resistivity of the host lattice, ρ_0 , plus the resistivity of the defects, $\Delta\rho$. This is written as

$$\rho = \rho_0 + \Delta\rho \quad (5)$$

and is known as Matthiesen's rule.¹² The electron-diffusion thermopower S_e of a metal containing a dilute concentration of defects is then given by

$$S_e = -S_0 \left(\frac{\partial \ln [\rho_0(\epsilon) + \Delta\rho(\epsilon)]}{\partial \ln \epsilon} \right)_\zeta, \quad (6)$$

where it follows that,

$$S_e = \frac{\rho_0}{\rho} S_e^0 + \frac{\Delta\rho}{\rho} S_e^i, \quad (7)$$

where

$$S_e^i = -S_0 \left(\frac{\partial \ln \Delta\rho}{\partial \ln \epsilon} \right)_\zeta, \quad (8)$$

and

$$S_e^0 = -S_0 \left(\frac{\partial \ln \rho_0}{\partial \ln \epsilon} \right)_\zeta. \quad (9)$$

S_e^0 is the electron-diffusion thermopower of the pure metal, and S_e^i is identified as the intrinsic electron-diffusion thermopower of the defect.

S_e is defined as

$$S_e \equiv S_e - S_e^0. \quad (10)$$

Then from Eqs. (7)–(10), we have

$$\Delta S_e = \frac{S_e^0}{\rho_0/\Delta\rho + 1} \left(\frac{\partial \ln \Delta\rho / \partial \ln \epsilon}{\partial \ln \rho_0 / \partial \ln \epsilon} + 1 \right)_\zeta. \quad (11)$$

Corrections for deviations from the Wiedemann-Franz law were not included since the approximations involved in the Nielsen-Taylor theory described below are more serious.

Nielsen and Taylor⁸ use a free-electron model and a Debye spectrum to develop a simple expression for the electron-diffusion thermopower of a metal. The electrical resistivity is written as

$$\rho(\epsilon) \propto 1/v^2(\epsilon)\tau(\epsilon)N(\epsilon), \quad (12)$$

where $\tau(\epsilon)$ is the electron relaxation time, $v(\epsilon)$ is the electron velocity, and $N(\epsilon)$ is the density of states. In a system of free electrons, both $v(\epsilon)$ and $N(\epsilon)$ are proportional to $\epsilon^{1/2}$. Thus we have

$$\left(\frac{\partial \ln \rho(\epsilon)}{\partial \ln \epsilon} \right)_\zeta = \left(\frac{\partial \ln(1/\tau)}{\partial \ln \epsilon} \right)_\zeta - \frac{3}{2} \quad (13)$$

or

$$\left(\frac{\partial \ln \rho_0}{\partial \ln \epsilon} \right)_\zeta = D_1 - \frac{3}{2}, \quad (14)$$

and

$$\left(\frac{\partial \ln \Delta\rho}{\partial \ln \epsilon} \right)_\zeta = D_2 - \frac{3}{2}, \quad (15)$$

where

$$D_i \equiv \left(\frac{\partial \ln(1/\tau_i)}{\partial \ln \epsilon} \right)_\zeta, \quad i = 1, 2. \quad (16)$$

The relaxation times τ_1 and τ_2 are for electron-phonon scattering and electron-impurity scattering, respectively. Equations (9) and (11) can now be rewritten as

$$S_e^0 = S_e^0 \left(\frac{3}{2} - D_1 \right) \quad (17)$$

and

$$\Delta S_e = \frac{S_e^0}{\rho_0/\Delta\rho + 1} \left(\frac{D_2 - \frac{3}{2}}{D_1 - \frac{3}{2}} - 1 \right). \quad (18)$$

Rearranging terms in Eq. (18) and making use of Eq. (17), one gets

$$\Delta S_e = \frac{S_0}{\rho_0/\Delta\rho + 1} (D_1 - D_2). \quad (19)$$

The major contribution of Nielsen and Taylor enters at this point through the calculation of D_2 . Dudenhoeffer and Bourassa used the pure metal experimental data for S_0^o (see Fig. 2) to compute D_1 via Eq. (17), and that method will also be used in this work. It was assumed that the plot of the diffusion thermopower of pure aluminum versus absolute temperature is a straight line with slope $-3.0 \times 10^{-3} \mu\text{V}/^\circ\text{K}^2$, as determined by Gripshover, Van Zytveld, and Bass.¹³

The expression for D_2 as calculated by Nielsen and Taylor⁸ is

$$D_2 = \frac{1}{2} + 2 \frac{\partial \ln \mathfrak{u}}{\partial \ln \epsilon} \Big|_{\epsilon} + \frac{9\mathfrak{u}}{4k_B T} \frac{m}{M} \frac{N'}{N} \Psi \left(\frac{T}{\Theta} \right) + \frac{2}{3} \frac{\mathfrak{u}\zeta}{4k_B T(k_B\Theta)} \frac{m}{M} \left(\frac{2N}{N'} \right)^{1/3} L_2 \left(\frac{2T}{\Theta} \right), \quad (20)$$

where Θ is the Debye temperature, N is the number of ions in the sample, N' is the number of free electrons in the sample, m/M is the ratio of electronic to ionic masses, \mathfrak{u} is the pseudopotential of the host, \mathfrak{u} is the renormalized pseudopotential appropriate to the dilute alloy, and $\Psi(T/\Theta)$ and $L_2(2T/\Theta)$ are complicated functions of temperature given in Ref. 8. Nielsen and Taylor⁸ have shown that the limit of high temperature D_2 reduces to the traditional temperature-independent result given by the first two terms in Eq. (20).

The value of \mathfrak{u} was obtained from the expression

$$\mathfrak{u}^2 = 4 \int_0^1 U^2(x) x^3 dx, \quad (21)$$

where

$$x = q/2k_F, \quad (22)$$

k_F being the Fermi radius, and

$$U(x) = (\Omega_2/\Omega_1) V_2(x) - V_1(x). \quad (23)$$

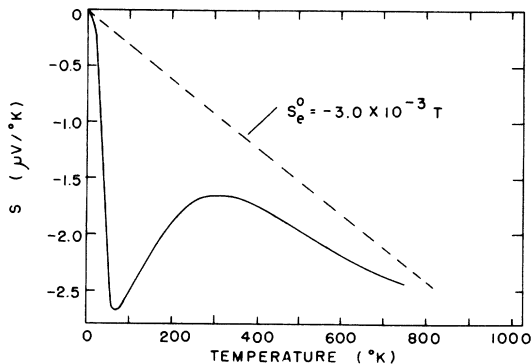


FIG. 2. Absolute thermopower curve for aluminum. (Taken from Gripshover, Van Zytveld, and Bass, Ref. 7.)

The quantities $V_1(x)$ and $V_2(x)$ are the pseudopotentials of the host and solute, respectively, calculated by Animalu and Heine,¹⁴ as quoted by Harrison¹⁵; the quantities Ω_1 , and Ω_2 are the atomic volumes of the host and the solute, respectively. The value of the pseudopotential $V_2(x)$ of the vacancy might reasonably be taken as an adjustable parameter, but in keeping with the simplicity of the model, i. e., free electron and Debye spectrum, the value of $V_2(x)$ has been assumed to be zero. Nielsen and Taylor⁸ developed the expression for \mathfrak{u}^2 given above. However, they took $U(x)$ to be constant and evaluated it at $x=0$. This can lead to large errors for some alloys. The sign of \mathfrak{u} was taken as the sign of the values of $U(x)$ which make the major contribution to \mathfrak{u} . The value used in this paper was 0.1 Ry.

Similarly \mathfrak{v} is obtained from the expression

$$\mathfrak{v}^2 = \frac{\int_0^{x_D} |V_1(x)|^2 x^4 \text{csch}(\Theta x/Tx_D) dx}{\int_0^{x_D} x^4 \text{csch}(x/Tx_D) dx}, \quad (24)$$

where $x_D = q_D/2k_F$, q_D being the Debye cutoff. This expression was developed by Nielsen and Taylor,⁸ although they again took $V_1(x)$ as a constant and removed it from the integral. The values used for \mathfrak{v} were temperature dependent and ranged from -0.55 to -0.38 Ry. The value of $\partial \ln \mathfrak{u} / \partial \ln \epsilon \Big|_{\epsilon}$ could have been adjusted to match ΔS_e with the total measured thermopower difference ΔS at high temperatures. This was not done because there is evidence¹³ in aluminum that the phonon-drag contribution to the thermopower is nonzero even at the melting point, and it certainly remains important at the highest temperature in this experiment, 150°K (see Fig. 2). Instead a simple screened Coulomb potential was used to express the energy dependence of \mathfrak{u} . The logarithmic derivative is then given by

$$\frac{\partial \ln \mathfrak{u}}{\partial \ln \epsilon} \Big|_{\epsilon} = -\frac{1}{2} - \frac{1}{2\epsilon(q)}, \quad (25)$$

where $\epsilon(q)$ is the Hartree dielectric function for aluminum as tabulated in Harrison.¹⁵ An average over q was taken, and that value used was $\partial \ln \mathfrak{u} / \partial \ln \epsilon \Big|_{\epsilon} = -0.72$.

The determination of ΔS_e was carried out and is presented in Sec. IV. The values of ΔS_e were then determined by subtracting ΔS_e from the total measured ΔS . These results are discussed in Sec. IV.

Estimation of the Rayleigh Scattering Parameter for Phonon Scattering from Vacancies

In a solid a defect of atomic dimensions, such as a vacant lattice site, will upset the regularity of the crystal lattice. At low temperatures this irregularity will be very much smaller than the phonon wavelength so that the scattering which it pro-

duces is analogous to the Rayleigh scattering in optics and atomic physics with the scattering probability proportional to the fourth power of the phonon wave vector q . It follows that the phonon-vacancy relaxation time τ ; is inversely proportional to the fourth power of the phonon frequency, the constant of proportionality being the Rayleigh scattering parameter a . The actual magnitude of the scattering will be determined by the difference in density and in elastic constant caused by the scattering center in the lattice.

Huebener¹⁶ using the results of several authors has obtained an expression for the change ΔS_g in phonon-drag thermopower; this expression includes the Rayleigh-scattering parameter a and is given by

$$\Delta S_g = -Ae^{\beta/T} \int_0^{\Theta/T} \frac{z^2 e^z}{e^z - 1} \left(1 + \frac{bh^2 e^{-\beta/T}}{ak_B^2 z^2 T} \right) dz, \quad (26)$$

where

$$z = \hbar\omega/k_B T;$$

and A , b , and β are constants determined empirically. This expression is used in this work to estimate the Rayleigh-scattering parameter and to indicate that the broad maximum in the thermopower curves found above 80 °K is most likely due to phonon drag.

The constants b and β were determined from the lattice thermal conductivity K_L , which is given by

$$K_L = \frac{k_B}{2\pi^2 v_s} \left(\frac{k_B T}{\hbar} \right)^3 \int_0^{\Theta/T} \frac{\tau_0 z^4 e^z}{e^z - 1} dz, \quad (27)$$

where v_s is the velocity of sound and τ_0 is the relaxation time for phonon scattering in the host material.

The form used for τ_0 was that used by Pohl and Walker¹⁷:

$$\tau_0^{-1} = b\omega^2 T e^{-\beta/T}. \quad (28)$$

The constant A was determined from Huebener's expression for the pure metal phonon-drag thermopower S_g^0 which is

$$S_g^0 = A e^{\beta/T} \int_0^{\Theta/T} \frac{z^2 e^z}{(e^z - 1)^2} dz. \quad (29)$$

The results of these calculations are presented in Sec. IV. The value of the scattering parameter a obtained in this way is to be compared with the values of a predicted by Klemen's theory¹⁸ and Carruthers's theory.¹⁹

Using second-order perturbation theory, Klemen obtained an expression for a :

$$a = (3\Omega c / \pi v_s^3) L^2, \quad (30)$$

where Ω is the atomic volume of the crystal, c is the mole fraction of the point defects, and

$$L^2 \equiv \frac{1}{12} \left(\frac{\Delta M}{M} \right)^2 + \left[\frac{1}{\sqrt{6}} \frac{\Delta F}{F} - \left(\frac{2}{3} \right)^{1/2} Q\gamma \frac{\Delta R}{R} \right]^2, \quad (31)$$

where γ is the Gruneisen constant, M is the atomic mass of the crystal, F is the force constant of a linkage, R is the nearest-neighbor distance, and Q is the contribution to the scattering matrix from strain outside the six nearest neighbors. Also, ΔM , ΔF , and ΔR are changes in the appropriate quantities at the sites of the point defects.

For strain-field scattering, Carruthers obtained the same relation as did Klemen, Eq. (30), but his expression for L^2 differed:

$$L^2 = 80 \gamma^2 (\Delta R/R). \quad (32)$$

III. EXPERIMENTAL APPARATUS AND PROCEDURES

Sample Preparation

Aluminum wire of 99.9999% purity was procured from Cominco American Inc., of Spokane, Washington. The specimen wires were 0.010-in. diameter, the holder wires were 0.018-in. diameter, and the wire forming the junctions were 0.005-in. diameter. Figure 3 shows the arrangement of the wires in the specimen.

In order to spot-weld aluminum it was necessary to acid etch the wires for 4 min in an 8% hydrofluoric acid solution, rinse off the acid in distilled water, and then rinse again in methanol. An Ewald welder, model WHDSA, was used to perform the spot welds.

The design of the sample holder was patterned after that of Huebener.¹⁶ The holder and its specimen consisted of a hot junction, a cold junction, a heater, a heat sink, and terminal blocks.

Since it provides good electrical insulation and high thermal conductivity yet is not attacked by methanol, Emerson and Cuming 2850 GT Stycast was used to coat the metal surfaces of the heat sink and heater. Apiezon *N* grease or Dow-Corning high-vacuum grease further improved the thermal conductivity and was used on all clamping surfaces. Stainless-steel tubing of 0.010-in. wall thickness was used in the frame.

It was not desirable to spot weld the sample after quenching since quenched-in vacancies in aluminum rapidly anneal out at room temperature. Instead a pressure junction was formed by clamping in a low-temperature liquid bath of methanol and dry ice. It was desired to determine the annealing temperature of the wire specimen. This was accomplished using 0.005-in. thermocouple wires spot welded at the two junctions before quenching, providing electrical contact for this measurement without creating significant heat sinks and resulting nonuniformity in temperature.

Two low-temperature electrical feedthroughs

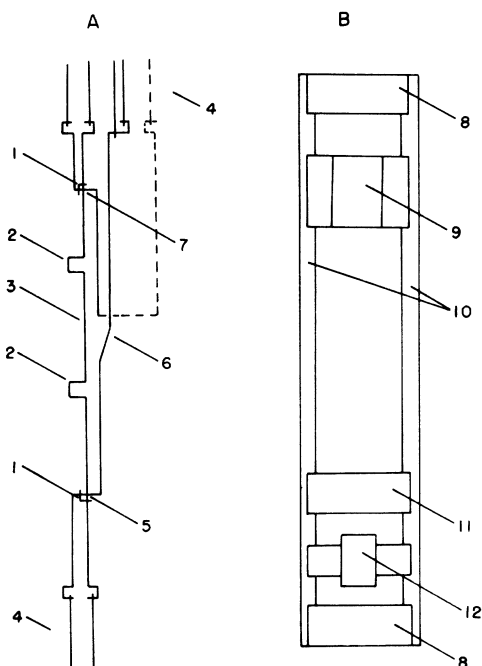


FIG. 3. (a) Specimen: (1) 0.005-in. junction wire, (2) expansion loop, (3) specimen wire, (4) holder wires, (5) lower junction, (6) well-annealed lead, (7) upper junction. (b) Sample holder: (8) terminals block, (9) heat sink, (10) thin-wall stainless-steel tubing, (11) thermocouple, (12) heater. Specimen and sample holder shown separately for clarity.

were fabricated following the design of Anderson.²⁰ These seals were still functioning satisfactorily after being thermally cycled many times and subjected to thermal shock. Note that the part of the wire which was in contact with the Stycast sealing compound was stripped of the insulative varnish to insure a better seal.

Annealing and Quenching Procedure

The specimen and the two potential lead wires were annealed by passing a direct current through them. It is estimated that the temperature along the length of the wire was uniform to $\pm 5\%$. The potential lead wires were heated at more than 525°C for $1\frac{1}{2}$ h. Over a period of 20 min the temperature was reduced continuously to approximately 150°C . The potential lead wires were then air quenched to room temperature to prevent formation of voids. The specimen wire was similarly heat treated and then annealed at the particular temperature of interest for $1\frac{1}{2}$ h before quenching. This heat treatment follows that used by Bass.²¹

The resistance of the specimen wire at room temperature was determined by measuring the voltage across the specimen as a known current passed through it. The resistance of the well-annealed

wire was also measured. This information was used to compute the annealing temperature prior to quench, T_Q , by comparing the resistivity of the specimen at temperature to the resistivity-versus-temperature data of Simmons and Balluffi.²²

The maximum value of current used in annealing was about 6 A. The annealing current value was obtained by measuring the voltage across a Leeds and Northrup 0.01- Ω standard resistance which was immersed in a stirred oil bath.

In quenching it is important that all parts of the wire enter the bath simultaneously and that the wire remain in motion while the wire is cooling to ensure a rapid quench.²³ Strain introduced in the wire during the quench can be minimized by making the distance of the specimen wire from the quench surface as small as possible, about 1 to 2 cm. It was found that expansion loops (see Fig. 3) reduce specimen distortion during annealing.

The specimen was quenched into a medium of distilled water and ice. The quench rate in this procedure was measured to be $2.5 \times 10^4^\circ\text{C}/\text{sec}$. Then the specimen was transferred from the ice and water bath into a second bath of dry ice and methanol at a temperature of -80°C . The transfer time from the water quench until the specimen was immersed in the cold methanol was less than 15 sec. This was an essential step because in aluminum the temperature should not exceed -80°C to insure that the quenched-in vacancies do not anneal out.

In his work on quenching in aluminum, Bass²¹ found no systematic differences between data taken on wires quenched to 0, -40 , or -50°C , provided that the wires were quickly (10 to 15 sec) immersed in liquid nitrogen.

After the specimen had been immersed in methanol, the hot and cold junctions and the heater unit were clamped in place in the cold liquid. A copper can with an indium O-ring in place was lowered into the methanol bath and allowed to cool. The sample holder, which was connected to the quench lever (see Fig. 4), and the specimen were inserted into the copper can. This operation was performed with the specimen wire at all times submerged in the cold methanol. The quenching leads and quench lever were removed.

After the vacuum O-ring seal was made, the liquid within the copper can was drained, and nitrogen gas was introduced into the can to inhibit atmospheric condensates from forming. The can was immersed in a liquid-nitrogen bath, evacuated, and finally inserted into a cryostat which had been precooled to liquid-nitrogen temperature.

Liquid helium was then introduced to reduce the sample temperature to 4.2°K .

In order to determine the vacancy concentration the resistances of the specimen and of the well-

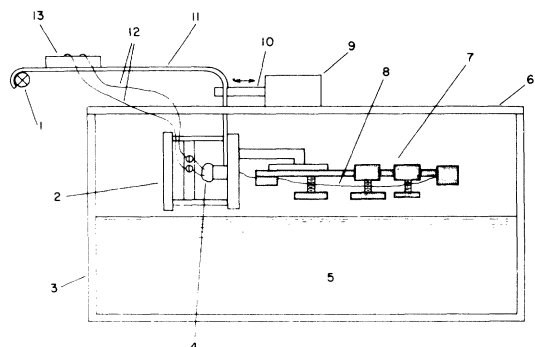


FIG. 4. Quench tank with quenching assembly: (1) pivot axis, (2) connecting vacuum plate, (3) five gallon aquarium tank, (4) electric feed through, (5) quenching medium, (6) cover, (7) specimen and holder, (8) heated specimen wire, (9) solenoid, (10) release bar, (11) quench lever, (12) quenching leads, (13) terminals.

annealed wire were measured at 4.2 °K. The residual resistance ratios of the specimen and of the well-annealed wire were obtained; then the resistivities of both of these wires were computed at 4.2 °K using the value of resistivity of aluminum at room temperature from Simmons and Balluffi,²² $\rho(20^\circ\text{C}) = 2.65 \mu\Omega \text{ cm}$. The quenched-in resistivity due to vacancies was calculated by subtracting the resistivity of the well-annealed wire from the specimen resistivity. Finally the vacancy concentration was determined using the Simmons and Balluffi value²² for the intrinsic resistivity of a vacancy in aluminum as $3 \times 10^{-6} \Omega \text{ cm/at.}\%$.

Measurement Procedures

A Guildline 9176-G nanovolt potentiometer was used to measure the very small thermovoltages of this work. It has a theoretical sensitivity of 10^{-9} V and in this application has given stable readings of 5×10^{-9} V. A Guildline 9461-A galvanometer and a Guildline 9460-A photoelectric nanovolt amplifier were used in association with the potentiometer.

A Leeds and Northrup Type K-4 potentiometer (with a sensitivity of 10^{-7} V) together with a Leeds and Northrup dc null detector were used to measure the hot-junction thermocouple voltages. The K-4 instrument was also used to monitor the heat-sink temperature.

The temperatures of the hot junction and the heat sink were monitored by two thermocouples (Fig. 5). The thermocouple wire was obtained from the Sigmund-Cohn Corporation. These thermocouple materials have been calibrated by the National Bureau of Standards of Boulder, Colorado.²⁴ One wire was gold plus 0.07-at.% iron, while the other was chromel. Both were 0.003-in. diameter and coated with teflon. The two wires were spot welded together and to a 0.0005-in.-thick copper foil, 0.5

by 1 cm. A phenolic wafer thermally insulated the junction and foil from the sample holder. Good thermal contact with the aluminum wire junction was aided by a coating of Apiezon N or Dow-Corning high-vacuum grease.²⁵ The change in temperature of the copper heat sink was measured to be a maximum of 1 °K during the experiment. This occurred when the temperature gradient along the sample reached its maximum value of 10 °K/cm. The voltage picked off from a motor-driven variable resistance supplied the heater current, which was reasonably linear with time. The experiment required a wide temperature range to be spanned within a few hours, since the liquid-helium boil-off rate limited the time available for measurement. The temperature was changed from 4.2 to 77 °K over a period of $5\frac{1}{2}$ h.

IV. RESULTS AND ANALYSIS

The thermoelectric voltage between the well-annealed wire and the specimen wire containing vacancies was measured as a function of hot-junction temperature. The difference in thermopower between the well-annealed wire and the specimen wire was found by taking the temperature derivative of the thermoelectric voltage curves using a seven-point quadratic fit. See Fig. 6, solid lines. The main characteristic of these curves is the pronounced negative minimum which occurs at approximately 30 °K. A second feature is the small broad positive maximum which occurs at approximately 90 °K. Thus the thermopower curves exhibit a double-humped shape. This shape is very similar to the dilute-alloy curves in aluminum obtained by Huebener,⁴ except that in the vacancy data the nega-

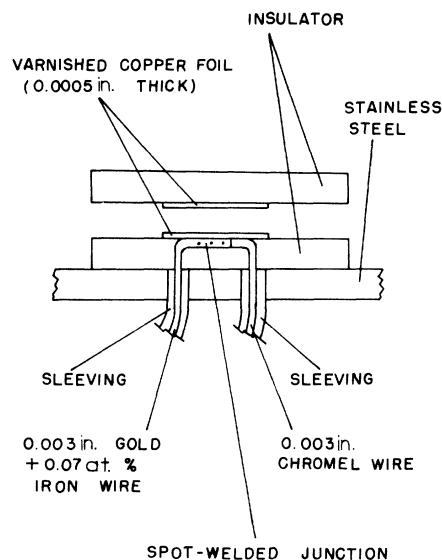


FIG. 5. Hot-junction thermometer arrangement.

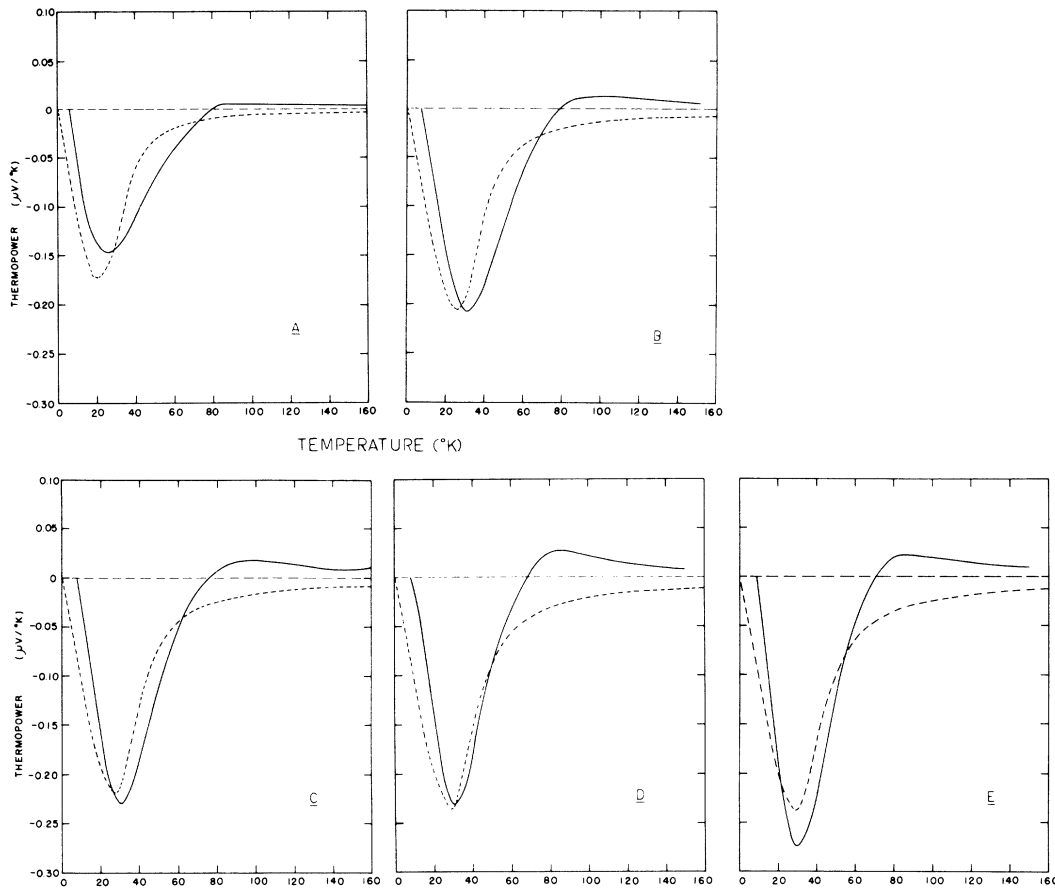


FIG. 6. Thermopower curves for vacancies in aluminum: (a) $T_Q = 416^\circ\text{C}$, $c = 0.852 \times 10^{-3}$ at.%; (b) $T_Q = 476^\circ\text{C}$, $c = 1.94 \times 10^{-3}$ at.%; (c) $T_Q = 538^\circ\text{C}$, $c = 2.36 \times 10^{-3}$ at.%; (d) $T_Q = 585^\circ\text{C}$, $c = 3.05 \times 10^{-3}$ at.%; (e) $T_Q = 555^\circ\text{C}$, $c = 3.48 \times 10^{-3}$ at.%. .

tive peak is much enhanced relative to the positive peak.

The dashed curves represent the theoretical electron-diffusion thermopower as computed from the Nielsen-Taylor theory. This calculation was discussed in Sec. II. Note the good agreement of the negative peak magnitudes and the location in temperature, especially for the high concentrations. No adjustable parameters have been used in this calculation.

For the samples the resistance ratio $R_{295^\circ\text{K}}/R_{4.2^\circ\text{K}}$ was measured to be from 1900 to 2400.

In order to identify the source of the broad maximum above 80°K , the Rayleigh-scattering parameter a is evaluated as outlined in Sec. II.

From the expression for the lattice thermal conductivity K_L in Eq. (27) and the expression for the inverse phonon scattering relaxation time τ_0^{-1} in Eq. (28), the constants b and β were evaluated as 4.0×10^{-8} sec/ $^\circ\text{K}$ and 62°K , respectively. The values used for the velocity of sound²⁶ and the Debye temperature were, respectively, 6.42×10^5 cm/sec and 428°K . The value for the lattice thermal con-

ductivity K_L was taken from White's table²⁷ as

$$K_L = 19/T \pm 50\% \text{ erg cm}^{-1} \text{ sec}^{-1} \text{ }^\circ\text{K}^{-1}. \quad (33)$$

Next, the constant A was determined in the expression for S_g^0 (Eq. 29). The value used for S_g^0 was taken from the graph of Griphover, Van Zytveld, and Bass¹³ at 100°K as $-2.16 \mu\text{V}/^\circ\text{K}$; see Fig. 2. The result is $A = -0.40 \mu\text{V}/^\circ\text{K}$.

In order to determine the scattering parameter a from Eq. (26) experimental values of ΔS_g at 100°K are needed. These values were obtained by subtracting the calculated value of ΔS_g from the experimental value of ΔS in each case [see Eq. (2)]. These scattering parameters obtained for each quench temperature T_Q are listed in Table I.

It is worthwhile to compare these experimental values with the values obtained from the theories of Klemens and Carruthers (see Sec. II). Using the atomic volume of the crystal for aluminum as 16.53×10^{-24} cm³, one obtains from Eq. (30)

$$a/c = 6.0 \times 10^{-43} L^2 \text{ sec}^3 / \text{at.} \% . \quad (34)$$

TABLE I. Scattering parameters for quench temperatures T_Q .

Quench temperature T_Q (°C)	$\Delta\rho$ ($10^{-9} \Omega \text{ cm}$)	a/c ($10^{-43} \text{ sec}^3/\text{at.}\%$)
416	2.56	16.4
476	5.83	18.7
538	7.07	20.3
585	9.15	19.9
555	10.45	18.3

In Klemens's theory the expression for L^2 is given by Eq. (31). Klemens states that for vacancies $\Delta M/M = -1$, $\Delta F/F = -1$, and $Q = 3.2$. From White,²⁷ $\gamma = 2.35$. It is also necessary to obtain the relative change in the nearest neighbor distance, $\Delta R/R$. From Butcher, Hutto, and Ruoff,²⁸ the activation volume of a vacancy is $\Delta V = 22 \times 10^{-24} \text{ cm}^3$, which implies a vacancy radius of $(\Delta V)^{1/3} = 2.80 \times 10^{-8} \text{ cm}$. The atomic volume for an aluminum ion, ΔV_{Al} is taken from Kittel²⁹ as 16.95×10^{-24} so that $(\Delta V_{Al})^{1/3} = 2.57 \times 10^{-8} \text{ cm}$. Following Klemens one obtains $\Delta R/R = +0.041$. L^2 is calculated to be 0.52 and from these values

$$a/c = 3.1 \times 10^{-43} \text{ sec}^3/\text{at.}\% . \quad (35)$$

From Carruthers's theory, using Eq. (32) one obtains

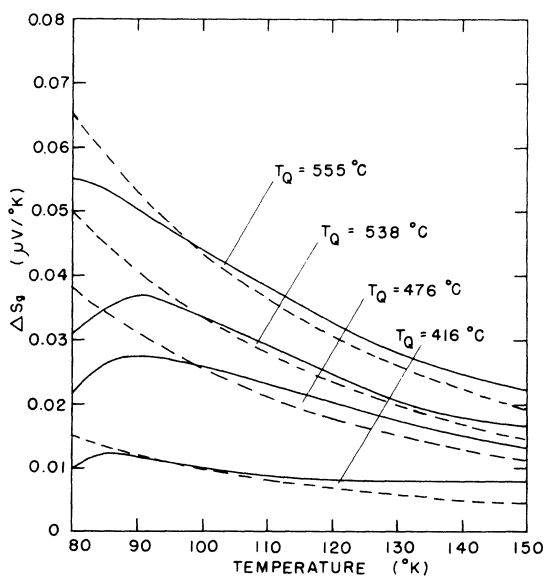


FIG. 7. Change in phonon-drag thermopower temperature dependence curves. Solid lines are the values of ΔS_g determined by subtracting the Nielsen-Taylor value of ΔS_e from the measured total change in thermopower, ΔS . Dashed lines are computed from Eq. (26).

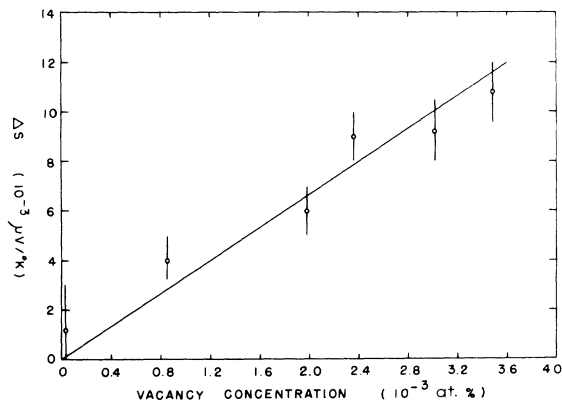


FIG. 8. Change in thermopower of aluminum at 150 °K versus quenched-in vacancy concentration.

$$a/c = 4.4 \times 10^{-43} \text{ sec}^3/\text{at.}\% . \quad (36)$$

The change in phonon-drag thermopower as calculated by subtracting the Nielsen-Taylor electron-

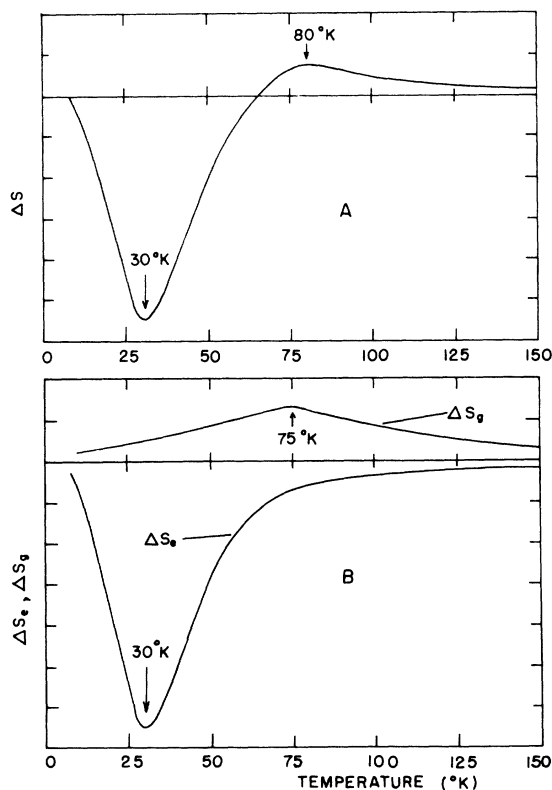


FIG. 9. Proposed resolution of the total change in thermopower into the electron-diffusion and phonon-drag components: (a) shows schematically the double-humped form of the ΔS curve; (b) shows schematically the proposed curves of the thermopower components ΔS_e and ΔS_g .

diffusion component from the total thermopower is shown in Fig. 7. The temperature dependence of the theoretical expression for ΔS_x obtained from Eq. (26) has been evaluated and also has been plotted on Fig. 7 (dashed lines) for comparison purposes. These theoretical values have been normalized to the experimental values at 100 °K. The curve for $T_Q = 585$ °C is not shown because it follows the curve for $T_Q = 555$ °C closely.

The change in thermopower ΔS in Fig. 8 varies linearly with concentration within the experimental accuracy of the data. Indirect evidence³⁰ indicates that the slope for aluminum vacancies might be anomalously high, but this has not been found in this work. The slope of the plot gives

$$(\Delta S/c)_{150^\circ\text{K}} = 3.3 \pm 0.5 \mu\text{V}/^\circ\text{K at.}\% . \quad (38)$$

V. DISCUSSION AND CONCLUSION

It is proposed that the double-humped curve of thermopower of vacancies be resolved into two components. This is shown schematically in Fig. 9. The negative minimum at 30 °K is due to the electron-diffusion thermopower and the positive maximum near 85 °K is due to phonon-drag thermopower.

It is apparent, in fact, from Fig. 6 that the Nielsen-Taylor theory predicts a negative minimum of the same magnitude and occurring at approximately

the same temperature as the experimentally obtained curves. This successful prediction of the peak temperature was also found by Dudenhoefter and Bourassa¹¹ in the case of aluminum alloys. The concentration spanned by the vacancy data and the alloy data is from 0.33×10^{-4} to 0.5 at.%. Caution is advised in concluding that the Nielsen-Taylor idea has replaced the phonon-drag interpretation of enhancement. Both theories need to be refined further before such a conclusion can be reached. Perhaps the truth will contain contributions from both.

There is also evidence that the positive maximum in ΔS is the expected reduction of the phonon-drag component of thermopower due to the vacancies. This evidence comes from the calculation of the Rayleigh-scattering parameter a . The experimental determination of this parameter gives values consistent with the values calculated from the theoretical expressions of Klemens¹⁸ and Carruthers.¹⁹ In addition, the temperature dependence of the change in phonon-drag thermopower due to vacancies in aluminum has been calculated using the theoretical expressions of Huebener.¹⁶ The agreement with the experimental data indicates that the phonon drag component is dominant in this temperature range. These calculations were also made on two of the alloy curves of Huebener⁴ and the results are consistent with the proposed explanation.

*Work supported in part by the Atomic Energy Commission, Contract No. AT-(40-1)3940. A grant from the Research Corporation made preliminary work on this project possible.
¹T. Farrell and D. Greig, in *Proceedings of the Tenth International Conference on Low-Temperature Physics, Moscow, 1966*, (VINITI, Moscow, 1967).
²C. Van Baarle, *Physica (Utr.)* **33**, 424 (1967).
³A. M. Guenault, *Philos. Mag.* **15**, 17 (1967).
⁴R. P. Huebener, *Phys. Rev.* **171**, 634 (1968).
⁵R. Fletcher and J. S. Dugdale, in Ref. 1.
⁶M. Bailyn, *Phys. Rev.* **157**, 480 (1967).
⁷J. S. Dugdale and M. Bailyn, *Phys. Rev.* **157**, 485 (1967).
⁸P. E. Nielsen and P. L. Taylor, AEC Technical Report No. 65 Coo623, 1970 (unpublished).
⁹P. E. Nielsen and P. L. Taylor, *Phys. Rev. Lett.* **25**, 371 (1970).
¹⁰P. E. Nielsen and P. L. Taylor, *Phys. Rev. Lett.* **21**, 893 (1968).
¹¹A. W. Dudenhoefter and R. R. Bourassa, *Phys. Rev. B* **5**, 1651 (1972).
¹²A. Matthiessen, *Rep. Brit. Assoc.* **32**, 144 (1862).
¹³R. J. Gripshover, J. B. Van Zytveld, and J. Bass, *Phys. Rev.* **163**, 598 (1967).
¹⁴A. O. E. Animalu and V. Heine, *Phys. Rev.* **12**, 1249 (1965).
¹⁵W. A. Harrison, *Pseudopotentials in the Theory of Metals*

(Benjamin, New York, 1966).
¹⁶R. P. Huebener, *Phys. Rev.* **135**, A128 (1964).
¹⁷C. T. Walker and R. O. Pohl, *Phys. Rev.* **131**, 1433 (1963).
¹⁸P. G. Klemens, *Proc. Phys. Soc. Lond. A* **68**, 1113 (1955).
¹⁹P. Carruthers, *Rev. Mod. Phys.* **33**, 92 (1961).
²⁰A. C. Anderson, *Rev. Sci. Instrum.* **39**, 605 (1968).
²¹J. Bass, *Philos. Mag.* **15**, 717 (1965).
²²R. O. Simmons and R. W. Balluffi, *Phys. Rev.* **117**, 62 (1960).
²³J. E. Bauerle and J. S. Koehler, *Phys. Rev.* **107**, 1493 (1957).
²⁴L. L. Sparks, R. L. Powell, and W. J. Hall, NBS Report No. 9712, Boulder, Colorado (unpublished).
²⁵G. K. White, *Experimental Techniques in Low-Temperature Physics*, 2nd ed. (Oxford U. P., Oxford, 1968).
²⁶*Handbook of Chemistry and Physics*, 48th ed. (CRC, Cleveland, Ohio, 1967), p. E-37.
²⁷G. K. White, in *Proceedings of the Eighth Conference on Thermal conductivity* (Plenum, New York, 1969), p. 37.
²⁸B. M. Butcher, H. Hutto, and A. L. Ruoff, *Appl. Phys. Lett.* **7**, 34 (1965).
²⁹C. Kittel, *Introduction to Solid State Physics*, 4th ed. (Wiley, New York, 1971).
³⁰R. R. Bourassa, D. Lazarus, and D. A. Blackburn, *Phys. Rev.* **165**, 853 (1968).

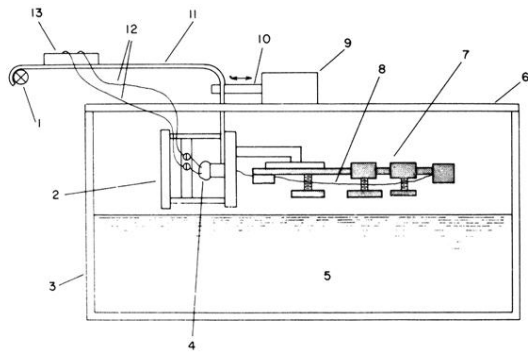


FIG. 4. Quench tank with quenching assembly: (1) pivot axis, (2) connecting vacuum plate, (3) five gallon aquarium tank, (4) electric feed through, (5) quenching medium, (6) cover, (7) specimen and holder, (8) heated specimen wire, (9) solenoid, (10) release bar, (11) quench lever, (12) quenching leads, (13) terminals.